

Vitamin D Receptor Expression in Plasmablastic Lymphoma and Myeloma Cells Confers Susceptibility to Vitamin D

Duncan M. Gascoyne,¹ Linden Lyne,¹ Hayley Spearman,¹ Francesca M. Buffa,² Elizabeth J. Soilleux,¹ and Alison H. Banham¹

¹Nuffield Division of Clinical Laboratory Sciences, Radcliffe Department of Medicine, and ²Department of Oncology, University of Oxford, Oxford OX3 9DU, United Kingdom

Plasmablastic B-cell malignancies include plasmablastic lymphoma and subsets of multiple myeloma and diffuse large B-cell lymphoma (DLBCL). These diseases can be difficult to diagnose and treat, and they lack well-characterized cell line models. Here, immunophenotyping and FOXP1 expression profiling identified plasmablastic characteristics in DLBCL cell lines HLY-1 and SU-DHL-9, associated with *CTNNB1*, *HPGD*, *RORA*, *IGF1*, and/or vitamin D receptor (VDR) transcription. We demonstrated VDR protein expression in primary plasmablastic tumor cells and confirmed in cell lines expression of both VDR and the metabolic enzyme CYP27B1, which catalyzes active vitamin D₃ production. Although *Vdr* and *Cyp27b1* transcription in normal B cells were activated by interleukin 4 (IL-4) and CD40 signaling, respectively, unstimulated malignant plasmablastic cells lacking IL-4 expressed both VDR and CYP27B1. Positive autoregulation evidenced intact VDR function in all plasmablastic lines, and inhibition of growth by active vitamin D₃ was both dependent on MYC protein inhibition and could be enhanced by cotreatment with a synthetic ROR ligand SR-1078. Furthermore, a VDR polymorphism, *FOK1*, was associated with greater vitamin D₃-dependent growth inhibition. In summary, HLY-1 provides an important model of strongly plasmablastic lymphoma, and disruption of VDR pathway activity may be of therapeutic benefit in both plasmablastic lymphoma and myeloma. (*Endocrinology* 158: 503–515, 2017)

The most common mature B lymphoma, diffuse large B-cell lymphoma (DLBCL), exhibits substantial heterogeneity in putative cell of origin and response to therapy and includes germinal center and activated B-cell (ABC)-like subtypes, the latter with poorer prognosis (1). A proportion of conventional ABC-DLBCLs exhibit overt plasmablastic characteristics, including major histocompatibility class II loss (2). These are recognized as having intermediate characteristics between DLBCL and plasmablastic lymphoma (PBL) (3, 4). PBL shares sufficient characteristics with plasmablastic myeloma to present a diagnostic challenge, and these malignancies likely represent a biological continuum, sometimes only distinguishable by means of detailed

clinicoradiopathological correlation (3, 4). The World Health Organization plasmablastic lymphoma category includes both HIV-associated, generally Epstein-Barr virus-positive PBL, found particularly in the oral cavity, and HIV⁻ PBL. PBL is frequently unresponsive to conventional DLBCL and myeloma therapies, conferring a dismal prognosis (4–7), and plasmablastic biology is poorly understood.

During plasma cell differentiation, expression of B-cell transcription factors FOXP1 and PAX5 alongside surface molecules CD19, major histocompatibility class II (HLA-DR), CD79a and CD79b, and CD20 is lost, whereas transcription factors IRF4, XBP1s, PRDM1, and surface markers CD38 and CD138 are induced

ISSN Print 0013-7227 ISSN Online 1945-7170

Printed in USA

Copyright © 2017 by the Endocrine Society

This article is published under the terms of the Creative Commons Attribution-NonCommercial License (CC-BY-NC; <https://creativecommons.org/licenses/by-nc/4.0/>).

Received 28 October 2016. Accepted 19 December 2016.

First Published Online 21 December 2016

Abbreviations: ABC, activated B cell; DLBCL, diffuse large B-cell lymphoma; IL, interleukin; PBL, plasmablastic lymphoma; VDR, vitamin D receptor; VitD₃, 1 α ,25-dihydroxyvitamin D₃.

(8–10). By definition, plasmablastic malignancies retain most characteristics of their normal counterparts (CD45⁺CD20⁺PAX5⁺CD138⁺CD38⁺Vs38c⁺XBP1S⁺). Despite gene expression profiling of normal human plasma cell development yielding insight into the biology of specific developmental stages (8, 9), progress in understanding malignant plasmablast biology is impaired by a paucity of characterized plasmablastic cell lines (11, 12).

Expression and function of the nuclear hormone receptor vitamin D receptor (VDR) are best characterized in bone, but VDR expression can be induced in B cells by interleukin (IL)–4 stimulation (13–16). Functionally, lipophilic ligands, including 1 α ,25-dihydroxyvitamin D3 (VitD3), which binds to nuclear VDR to regulate transcription, can inhibit plasma cell production (17) and growth of a subset of human B cells (15) and myeloma cells (18, 19). Studies have identified VDR expression in some mature B-cell lymphomas (20–22), although pathways inducing expression remain unclear, as is the importance of VDR polymorphisms such as *FOK1* (23–25). Multiple but conflicting studies have indicated vitamin D deficiency as a risk factor and/or prognostic indicator in non-Hodgkin lymphoma (26–31).

Here, we use immunophenotyping and FOXP1 expression to identify plasmablastic lymphoma and myeloma cell lines, including the strongly plasmablastic cell line HLY-1, and show that they have robust VDR expression. We demonstrate that VDR pathway activation can inhibit lymphoma cell growth and induce drug sensitivity and that *FOK1* polymorphism is associated with increased responses to VitD3. Thus, we provide insight into malignant plasmablastic biology and identify the VDR pathway as a potential therapeutic target.

Materials and Methods

Cell culture

Human DLBCL and myeloma cell lines were cultured in RPMI supplemented with 10% fetal bovine serum (Life Technologies, Paisley, UK). They were confirmed to be mycoplasma free, and their identity was validated by short tandem repeat profiling (LGC Standards, Teddington, UK). Murine CD43⁺ naive splenic B cells were purified from 5-week-old female C57BL/6 as per the manufacturer's protocols (Miltenyi Biotech, Cologne, Germany) and cultured in Iscove's modified Dulbecco medium containing 5% calf serum (Sigma, Gillingham, UK), 50 μ M 2-mercaptoethanol, 1 \times nonessential amino acids, and 1 \times penicillin/streptomycin/amphotericin B (Life Technologies) with or without α -immunoglobulin M (20 μ g/mL; eBioscience, Hatfield, UK), α -CD40 (2 μ g/mL; eBioscience), or recombinant murine IL-4 (10 ng/mL; Peprotech, London, UK). All VitD3 treatment experiments were initiated at 2×10^5 cells/mL in 24-well dishes, unless stated otherwise, using VitD3 (Sigma) dissolved in ethanol. The CDK4/6 inhibitor Palbociclib (PD-0332991)–HCL was supplied by Selleckchem

(Houston, TX) and 10058-F4 by Sigma. Epstein-Barr encoding region *in situ* hybridization was performed using a fully automated BondMax as per the manufacturer's instructions (Leica Bioscience, Newcastle, UK).

Colony formation assay

In total, 6×10^3 cells were plated into semisolid media (H4230; Stem Cell Technologies, Cambridge, UK) in 35-mm dishes and cultured for 7 days. Cell clusters were visually scored as colonies if at least 50 cells were present.

Viability and proliferation assays

Cells were cultured with either vehicle, and/or VitD3 (final concentration 10^{-7} M; Sigma), and/or ROR α/γ modulator SR-1078 (5 μ M; Merck-Millipore, Watford, UK). Transfection in the presence of 1 μ M Stealth siRNA duplexes (Life Technologies; Supplemental Table 1) was performed by electroporation (Amaxa Nucleofector Lonza, Slough, UK). After 24, 48, or 72 hours, cells were subjected to trypan blue viability assay, cytospin for hematoxylin and eosin stain (Sigma), MTS assay for total viable cell number (Promega, Southampton, UK), Annexin V/propidium iodide stain for apoptosis quantitation (BD Biosciences, Oxford, UK), and/or BrdU proliferation assay as per the manufacturer's protocols (BD Biosciences). Statistical significance was determined by Student *t* test.

Flow cytometry

Cells were stained in phosphate-buffered saline containing 0.5% bovine serum albumin, 2 mM EDTA, and specific antibodies (Supplemental Table 1) and analysis performed using FACSCalibur (BD Biosciences).

Protein detection by immunohistochemistry and immunoblotting

Cell pellets were formalin-fixed, sectioned, and paraffin-embedded slides dewaxed and antigen retrieved by microwaving in 50 mM Tris and 2 mM EDTA (pH 9.0). Immunostaining was performed with appropriate isotype or primary antibodies (Supplemental Table 1), followed by Envision detection (Dako, Ely, UK). For double labeling, immunostaining was repeated using a second primary antibody and blue substrate (Vector SG; Vector Laboratories, Peterborough, UK). Plasmablastic lymphomas and plasmablastic myelomas were defined according to current World Health Organization criteria, samples were collected with informed consent in accordance with the Declaration of Helsinki, and these studies were performed under local ethical approval from Oxford University (04/Q1604/21). Stained sections were scored independently by two authors (A.H.B. and E.J.S.) for VDR subcellular localization, the frequency of VDR positivity (10% increments), and the intensity of staining (negative, weak, moderate, or strong, scored as 0 to 3). For immunoblotting, whole-cell extracts were subjected to sodium dodecyl sulfate–polyacrylamide gel electrophoresis and probed using specific antibodies (Supplemental Table 1). Blots were routinely incubated overnight in phosphate-buffered saline containing 5% milk and 0.02% Tween-20, and signals were detected using ECL reagent (GE Healthcare, Little Chalfont, UK). β -Actin or nucleophosmin detection controlled for sample loading and transfer. Band intensities were determined by ImageJ quantitation, and expression of test proteins was

semiquantitated by normalization against band intensity of the relevant loading control β -actin.

VDR polymorphism analysis

The 5' and 3' VDR coding regions were amplified from cell line complementary DNA using GoTaq (Promega) with primers complementary to exons 2 to 7 and 6 to 10, and fragments were cloned into pGEM-Teasy (Promega) and subjected to sequencing analysis (Supplemental Table 1).

Gene expression analysis

Total RNA was isolated using a spin column (Qiagen, Manchester, UK), and random-primed complementary DNA was prepared using Superscript III (Life Technologies). Real-time polymerase chain reaction was performed on a Chromo4 machine (BioRad, Herts, UK) using Express qPCR supermix (Life Technologies) and Taqman assays (Life Technologies; Supplemental Table 1). Expression was normalized against *18S*, *TBP*, *PGK*, *β 2M*, *POL2RA*, *HPRT*, *ACTB*, and/or *GAPDH*; data shown are *18S* normalized unless indicated otherwise. Analysis of published microarray data (32) was performed using R software (<https://www.r-project.org/>) or Microsoft Excel. Genes whose expression correlated significantly with that of VDR (204255_s_at) were identified using a lymphoma data set (33) and compared with the previously identified stroma gene signature stromal 1 (33).

Results

Reduced FOXP1 expression and immunophenotyping identify plasmablastic lymphoma/myeloma cell lines

FOXP1 protein is expressed in ABC-DLBCL (32) and normal B-cell subsets (34) but generally not in myeloma or normal plasma cells (10). Thus, we hypothesized that comparatively weak FOXP1 protein expression in ABC-DLBCL might identify a more plasmablastic phenotype. Although gene expression profiling classifies the cell line HLY-1 as ABC-DLBCL (32), it has less FOXP1 protein (32) and transcript than "classic" ABC-DLBCL cell lines such as HBL-1 and OCI-Ly3 (Supplemental Fig. 1A and B). Notably, HLY-1 is CD138⁺ and expresses neither CD19 nor CD79b and has reduced surface HLA-DR compared with other ABC-DLBCL cell lines [Fig. 1(a)]. HLY-1 demonstrates reduced *PAX5* and increased *XBP1* and *PRDM1* expression with atypical coexpression of CD138 and FOXP1 in individual cells, which have a high nuclear to cytoplasmic ratio and are almost exclusively CD20[−] [Fig. 1(b) and 1(c)]. Rare, strongly FOXP1-positive cells are CD138[−] [Fig. 1(c), arrow]. HLY-1 was found to be Epstein-Barr virus negative by *in situ* hybridization for Epstein-Barr encoding region (Supplemental Fig. 1C). An apparent differentiation block at a more advanced stage of B-cell development may explain why, although HLY-1 is sensitive to MYD88 inhibition as per ABC-DLBCL cell lines (35), it is unusually MALT-1 independent (36) and extremely sensitive to bromodomain inhibition (37).

DLBCL, plasmablastic lymphoma, and plasmablastic myeloma likely represent a developmental continuum. Accordingly, an additional ABC-DLBCL cell line, SU-DHL-9, exhibited reduced surface HLA-DR and CD79b and slightly reduced *PAX5* compared with HBL-1 [Fig. 1(a) and 1(b)], whereas JJN-3 and Thiel myeloma lines showed increased surface HLA-DR alongside reduced *XBP1* and *PRDM1* expression in comparison with RPMI-8226 and NCI-H929 myeloma [Fig. 1(a) and 1(b)]. Thus, SU-DHL-9, HLY-1, JJN-3, and Thiel display varying degrees of plasmablastic character.

Expression of normal plasmablastic markers and VDR by DLBCL and myeloma cell lines

To examine the malignant plasmablastic phenotype further, we first identified plasmablast-associated genes from models of nonmalignant B-cell differentiation by cross-referencing two published gene expression data sets (8, 9). Three genes (*CTNNAL1*, *HPGD*, and *IGF1*) exhibited preferential expression in CD20^{lo} preplasmablasts, CD20[−] preplasmablasts, and plasmablasts, respectively, with an additional gene (*NRLP7*) showing expression in plasmablasts but also mature plasma cells (Supplemental Fig. 2A). Surprisingly, cell line expression patterns suggested conservation of plasmablastic differentiation subtyping, with SU-DHL-9, HLY-1, and JJN-3/Thiel appearing to express genes characterizing the earliest (*CTNNAL1*^{hi}), intermediate (*HPGD*^{hi}), and latest (*IGF1*^{hi}) stages of plasmablast development, respectively [Fig. 2(a)].

Analysis of published DLBCL cell line gene expression profiling (32) confirmed high expression of *IGF1*, *HPGD*, and *CTNNAL1* in HLY-1, and this data set was further interrogated for "receptor" annotated or cell surface protein-encoding genes potentially identifying therapeutic targets in plasmablastic malignancy. Although most genes highly expressed in HLY-1 were shared with the ABC-DLBCL cell lines OCI-Ly3 and OCI-Ly10, 21 probe sets representing 18 genes of potential interest were identified from the top 100 genes exhibiting preferentially high expression in HLY-1 [Fig. 2(b)]. High VDR expression was intriguing given the existing literature regarding VDR and vitamin D in lymphoma and myeloma (18–23, 26–31, 38) and upregulated VDR expression in normal plasmablastic cells (Supplemental Fig. 2B). High *RORA* was also initially interesting because a synthetic ligand for the *RORA*-encoded *ROR α* receptor can be toxic to tumor cells (39, 40), but *RORA* transcripts were not enriched in normal plasmablastic cells (Supplemental Fig. 2B) and absent from two of four lines with plasmablastic characteristics (Supplemental Fig. 2C). Importantly, three of these lines did exhibit robust VDR transcript and protein expression [Fig. 2(c)], which was

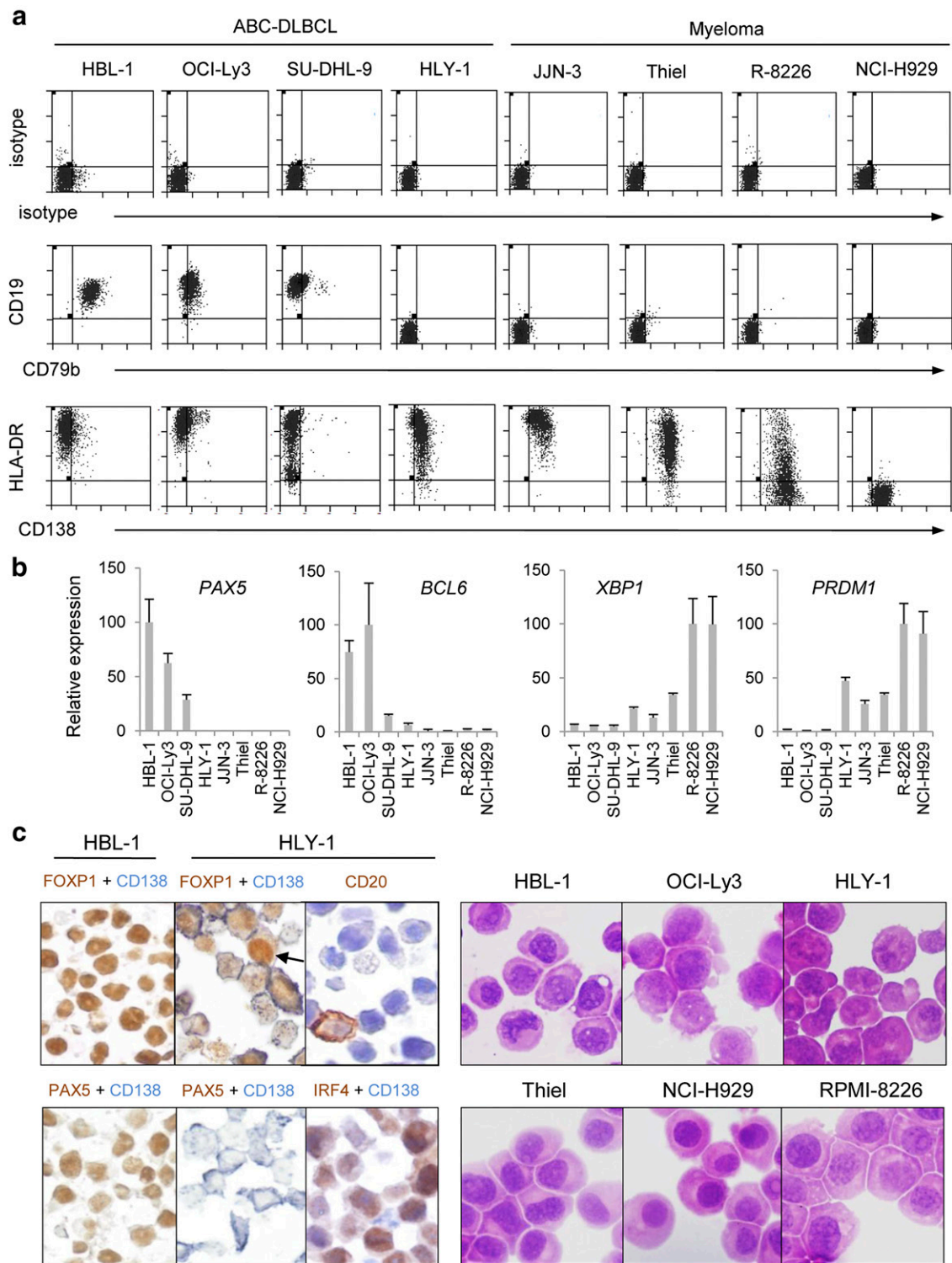


Figure 1. Reduced FOXP1 expression and immunophenotyping identify plasmablastic lymphoma/myeloma cell lines. (a) Surface flow cytometry of DLBCL and myeloma cell lines, representative of $n = 3$. (b) Real-time polymerase chain reaction of B-cell (*PAX5*) and plasma cell (*XBPA* and *PRDM1*) markers, relative to highest expressing line (100%), $n = 3 \pm$ SD. (c, left panels) Immunohistochemistry of FOXP1, CD138, CD20, PAX5, and IRF4, representative of two experiments. (c, right panels) Morphology of DLBCL and myeloma cell lines subjected to hematoxylin and eosin stain. SD, standard deviation.

associated with growth, because it could be reduced by either cell confluence or growth arrest induced by the CDK4/6 inhibitor palbociclib [Fig. 2(d)]. Mature myeloma lines also showed some VDR expression, and

targeted sequencing demonstrated that a slight increase in VDR protein mobility in NCI-H929 and HLY-1 [Fig. 2(c) and Supplemental Fig. 3A) was attributable to *FOK1* polymorphism (Supplemental Fig. 3B).

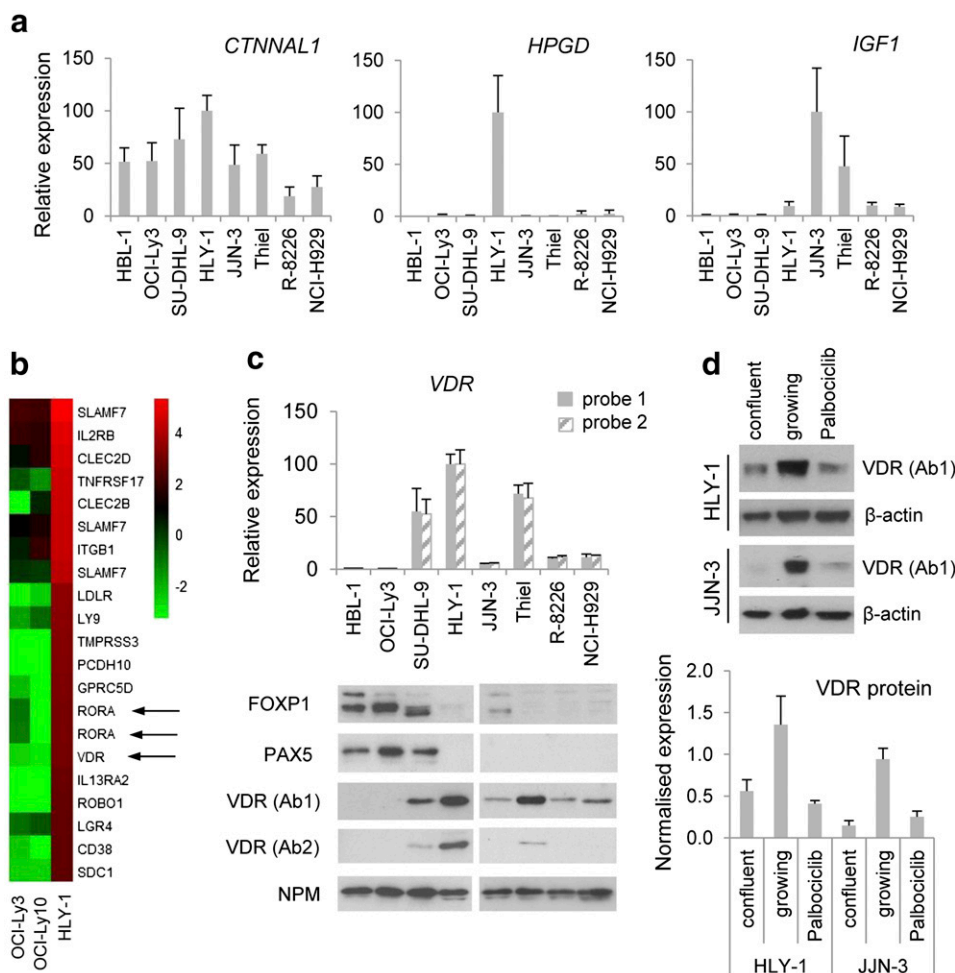


Figure 2. Expression of normal plasmablastic markers and VDR by DLBCL and myeloma cell lines. (a) Real-time polymerase chain reaction (PCR) of plasmablastic markers, relative to highest expressing line (100%), $n = 3 \pm$ SD. (b) Heat map showing Affymetrix probe set signals from DLBCL cell line gene expression profiling (32) identifying genes coding for cell surface proteins or with “receptor” annotation, having abundant expression in HLY-1 compared with OCI-Ly3 and OCI-Ly10, ranked by strength of expression in HLY-1. (c, upper panel) Real-time PCR of *VDR* transcript expression in lymphoma and myeloma lines relative to highest expressing line (100%), $n = 3 \pm$ SD, using two independent probes. (c, lower panels) Immunoblotting of FOXP1, PAX5, and VDR in the same cell lines. (d) Immunoblotting of VDR in cells exponentially growing or arrested by either saturating culture (confluent) or treatment of 48 hours with 1 μ M CDK4/6 inhibitor palbociclib; semiquantitative analysis of immunoblotting shown below as ratio of VDR to β -actin signal, mean \pm SE of duplicate experiments. SD, standard deviation; SE, standard error.

Primary plasmablastic lymphoma/myeloma tumor cells express nuclear VDR protein

Nuclear and cytoplasmic VDR protein expression in plasmablastic cell lines was confirmed by immunohistochemistry using anti-VDR antibody clone D6 (Ab1), a specific and sensitive reagent as described previously (41), notably demonstrating robust VDR expression in mitotic cells [Fig. 3(a)]. Importantly, this antibody detected nuclear VDR in five of eight primary plasmablastic tumors, with less frequent or no nuclear positivity observed in nonplasmablastic DLBCL tumors [Fig. 3(b) and Fig. 4(a)]. VDR protein was expressed also in some epithelia and other nontumor cells (such as Langerhans cells) on primary tumor sections [Fig. 3(b)]. Furthermore, VDR transcript expression associated with a stromal gene signature across a primary DLBCL series

(Supplemental Fig. 3C) suggests that total *VDR* transcript levels in lymphoma biopsy specimens may reflect not only tumoral but also nontumoral VDR expression. Nuclear VDR expression in primary plasmablastic tumors appeared in this cohort to be positively associated with proliferation determined by Ki-67 status [Fig. 4(b)].

Vitamin D levels determine VDR expression in plasmablastic tumor cells

Stimulation of normal human B cells can activate VDR expression and also that of *CYP27B1*, an enzyme catalyzing active VitD3 production from serum precursors. VDR is activated by IL-4, but the exact stimulus for *CYP27B1* is unclear (13, 14); furthermore, mechanisms regulating VDR expression in malignant

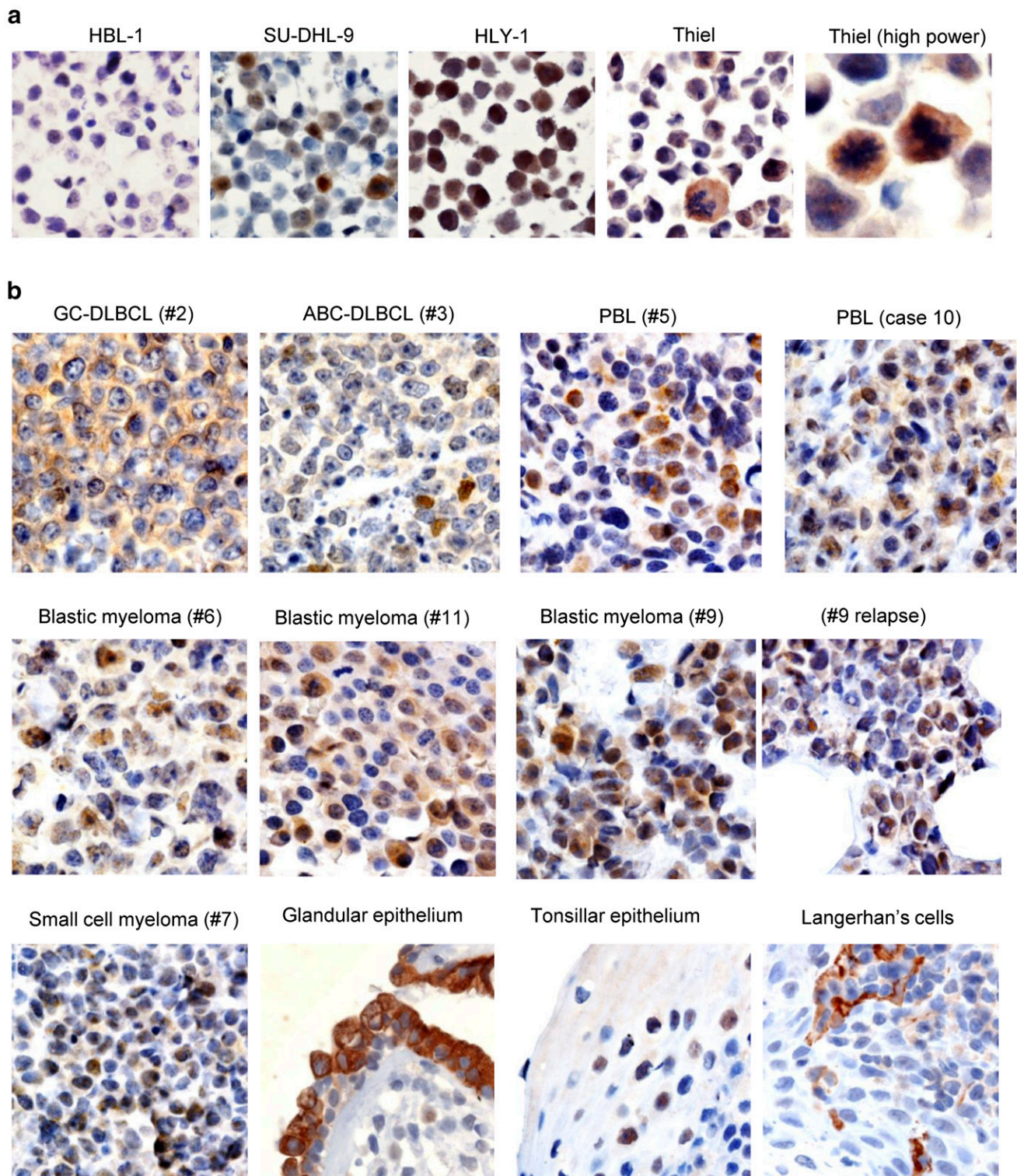


Figure 3. Primary plasmablastic lymphoma/myeloma tumor cells express nuclear VDR protein. Immunohistochemistry to detect VDR protein expression [antibody D-6 (Ab1) using a brown substrate, blue hematoxylin counterstain] in (a) cell lines, HBL-1 (negative, ABC-DLBCL), SU-DHL-9 (weakly plasmablastic DLBCL), HLY-1 (strongly plasmablastic ABC-DLBCL), and Thiel (plasmablastic myeloma), and in (b) primary plasmablastic tumors. Higher magnification in (A) right-hand panel highlights mitotic VDR expression.

B cells are uncharacterized. First, by activating naive murine B cells, we confirmed at both transcript and protein levels the IL-4 dependence of Vdr (both with and without α -CD40 costimulation) and demonstrated that Cyp27b1

is dependent primarily upon CD40 activation [Fig. 5(a)]. In contrast, plasmablastic tumor cells express VDR [Fig. 2(c)] in the absence of endogenous *IL-4* transcripts (data not shown) and abundant CYP27B1 in the absence of CD40

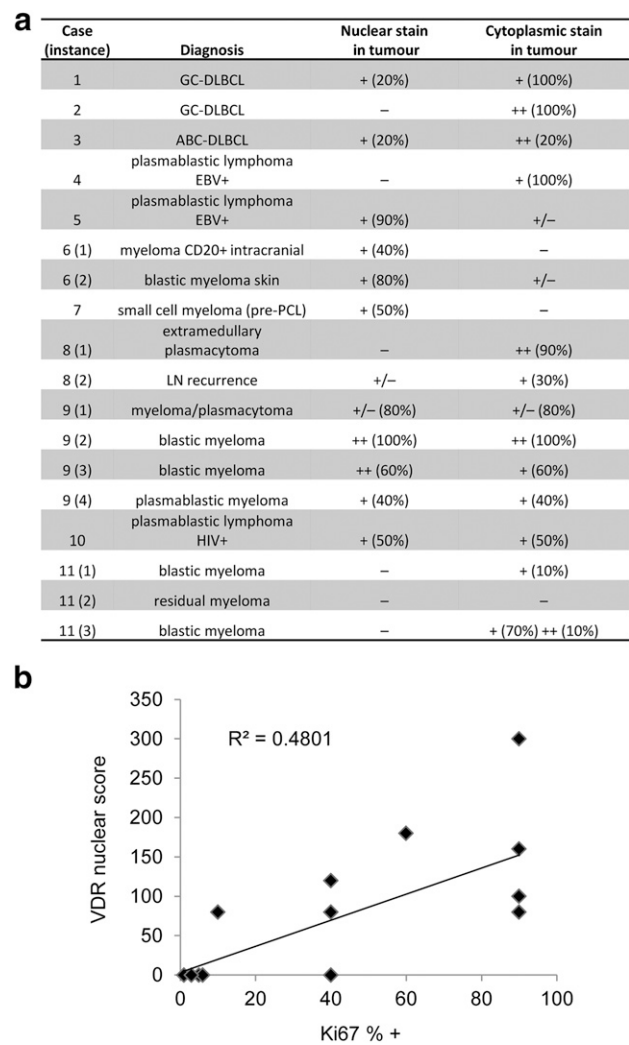


Figure 4. Primary plasmablastic lymphomas/myelomas express nuclear VDR protein associated with proliferative index. (a) Summary of VDR (antibody D-6) staining of primary lymphoma/myeloma cases. In some cases, sequential biopsy specimens from multiple presentations demonstrated maintained nuclear VDR expression throughout the disease course. Percentages indicate approximate proportion of tumor cells positively stained. (b) Nuclear VDR positivity was quantified approximately by multiplying stain intensity (–/±/+/++ as 0/1/2/3 respectively) by percentage of tumor cells stained and compared with percentage of Ki-67 positivity in tumor cells determined by clone MM1 immunohistochemistry.

ligation [Fig. 5(b)]. Thus, pathways regulating the vitamin D signaling loop appear distinct in normal B cells and plasmablastic tumor cells. CYP27B1 expression [Fig. 5(b)] and strong VDR autoregulation in VDR⁺ cell lines [Fig. 5(c)] indicate an intrinsic feed-forward VDR loop active in plasmablastic cells [Fig. 5(c)].

VDR expression promotes viability and susceptibility to VitD3-induced cell cycle inhibition

Exogenous VitD3 effects on lymphoma cells with minimal VDR expression are unclear (20, 42), and in our preliminary experiments, VDR[–] cell lines such as HBL-1 showed no significant growth responses to VitD3 (data not

shown). In contrast, VitD3 reduced viability of both plasmablastic DLBCL cell lines (HLY-1 and SU-DHL9) by significantly reducing proliferation [Fig. 6(a)]. Profiling of control and cell cycle-associated transcripts in VitD3 or vehicle-treated cells suggested a modest but broad effect on cell cycle regulators (Supplemental Fig. 4A and 4B), whereas expression of the classic VitD3 response gene *CYP24A1* was weakly induced by VitD3 (data not shown). Downregulated expression of cyclins A2, B2, E1, Rb, and, to a lesser extent, CDK4 was confirmed in HLY-1 cells by immunoblotting [Fig. 6(a)] and accompanied by MYC downregulation, as shown previously in HL-60 (43). Inhibition of MYC using 10058-F4 was sufficient to inhibit growth and decrease cyclin and CDK4 expression [Fig. 6(b)], indicating its important role in the vitamin D response. Interestingly, also VDR expression was reduced following MYC inhibition, evidencing a potential feed-back loop between VDR and MYC. Dose-response experiments showed that although MYC downregulation was not transcriptional, physiological VitD3 levels were sufficient to induce *IL6* transcription [Fig. 6(c)]. In contrast to active vitamin D (VitD3), treatment of HLY-1 and SU-DHL-9 with 10^{–7} M inactive precursor vitamin D (25D) did not inhibit growth (data not shown), suggesting that CYP27B1 activity in plasmablastic cells may be limiting. Interestingly, VDR depletion, which should inhibit VitD3 signaling, also decreased viability, demonstrating an additional role for the intrinsic VDR pathway [Fig. 6(d)]. Of three myeloma cell lines with similar VDR protein expression, NCI-H929 with the *FOK1* polymorphism displayed the most significant growth inhibitory response to VitD3 (Supplemental Fig. 4C).

VitD3 effects on plasmablastic cells can be enhanced by the synthetic ROR ligand SR-1078

Growth-inhibitory effects of VitD3 on plasmablastic lymphoma cell lines were significant but modest; therefore, potential sensitization to an additional drug was investigated. Having detected *RORA* expression in plasmablastic cell lines HLY-1 and JJN-3 (Supplemental Fig. 2C), we tested VitD3 in combination with the synthetic ROR ligand SR-1078 (39, 40). Strikingly, combined treatment produced an additive reduction in suspension culture viability and a synergistic decrease in colony formation [Fig. 7(a)]. A growth-inhibitory response to VitD3 alone was significant in HLY-1 but not in JJN-3, in accordance with lower basal VDR expression. Conversely, a significant response to SR-1078 alone was detected in JJN-3 but not in HLY-1 [Fig. 7(a)]. Mechanistically, combined drug effects were associated with greater growth inhibition in HLY-1 [Fig. 7(b)] and dramatic apoptosis in JJN-3 [Fig. 7(c)]. Altered surface

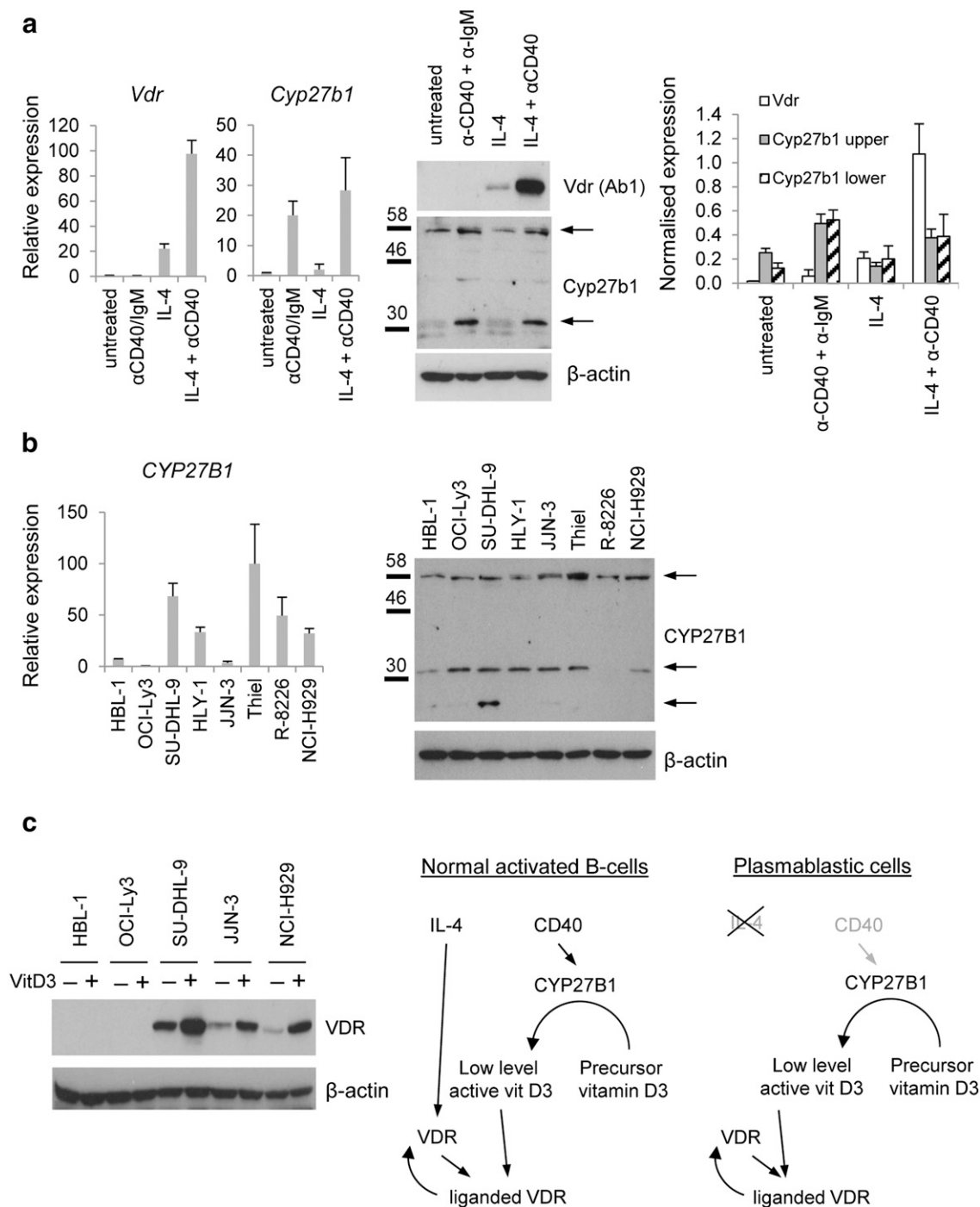


Figure 5. Vitamin D levels determine VDR expression in plasmablastic tumor cells. (a, left panels) Real-time polymerase chain reaction (PCR) of *Vdr* and *Cyp27b1* transcripts in 24-hour stimulated murine naive B-cell cultures relative to T = 0 untreated sample, $n = 2 \pm$ SE. (a, center panel) Immunoblotting of Vdr and Cyp27b1 in parallel T = 0 untreated or 48-hour stimulated cultures. (a, right panel) Semiquantitative analysis of immunoblots, mean \pm SE. (b) Real-time PCR of *CYP27B1* and CYP27B1 immunoblotting in lymphoma and myeloma cell lines; real-time transcript expression relative to highest expressor. (c, left panel) VDR immunoblotting of cell lines treated 24 hours with 10^{-7} M VitD3 (+) or ethanol vehicle (–). (c, right panels) Schematic of VDR regulation in normal and plasmablastic cells. SE, standard error.

CD138, HLA-DR, and CD38 expression, alongside rapid changes in *XBPI*, *CTNNAL1*, *PRDM1*, and *IGF1* transcription (Supplemental Fig. 5A and B; *PRDM1* confirmed at protein level), indicates that combined VitD3 and SR-1078-dependent toxicity in JJN3 cells results from disrupted plasmablastic identity.

In summary, VDR is expressed in normal and malignant plasmablastic cells, including those lacking overt plasmablastic characteristics. Greater understanding of VDR function, and potentially its manipulation in combination with other therapeutic strategies, may lead to novel treatments for plasmablastic lymphoma and myeloma.

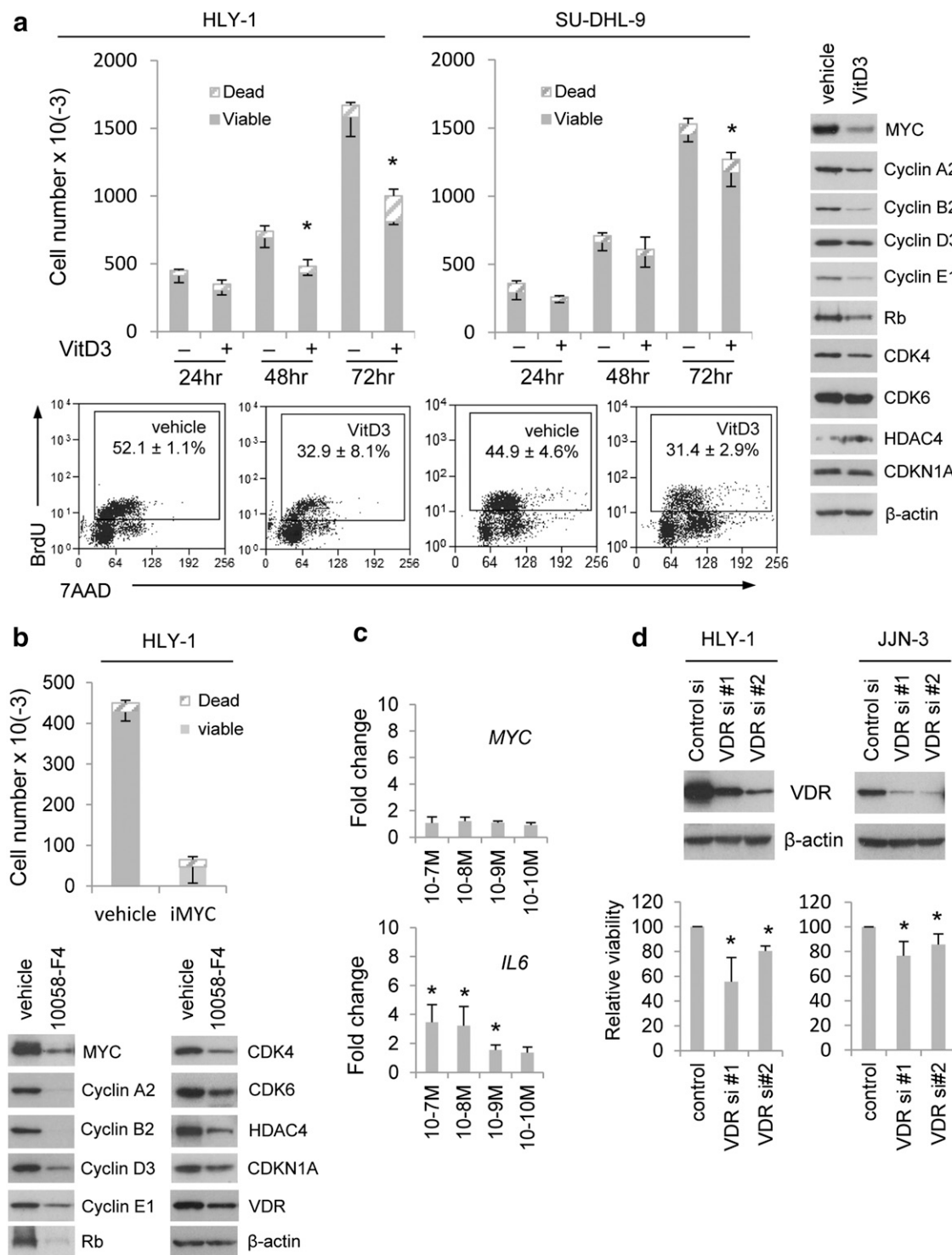


Figure 6. VDR expression promotes viability and susceptibility to VitD3-induced cell cycle inhibition. (a, left panels) Number of trypan blue-positive (Dead) and -negative (Viable) HLY-1 and SU-DHL-9 cells after treatment with ethanol vehicle (-) or VitD3 (+, single 10^{-7} M dose at T = 0), n = 3 \pm SD, and representative flow cytometry of BrdU incorporation/7-aminoactinomycin D (7-AAD) DNA content of cells cultured similarly for 48 hours. Numbers indicate mean percentage BrdU⁺ from n = 3 \pm SD. (a, right panels) Immunoblotting of similarly treated HLY-1, representative of 2 experiments. (b) Analyses as performed in (a) on HLY-1 treated for 48 hours with 50 μ M c-Myc inhibitor 10058-F4 or DMSO vehicle. (c) Real-time polymerase chain reaction of *MYC* and *IL6* in HLY-1 treated for 24 hours with ethanol vehicle or indicated dose of VitD3, expressed as fold change relative to vehicle, n = 4 \pm SD. (d) Representative immunoblotting and relative viable cell number determined by MTS assay 48 hours after transfection with control or one of two independent small interfering RNAs targeting *VDR*, n = 3 \pm SD. SD, standard deviation. **P* < 0.05, comparisons to same time-point vehicle or control siRNA sample.

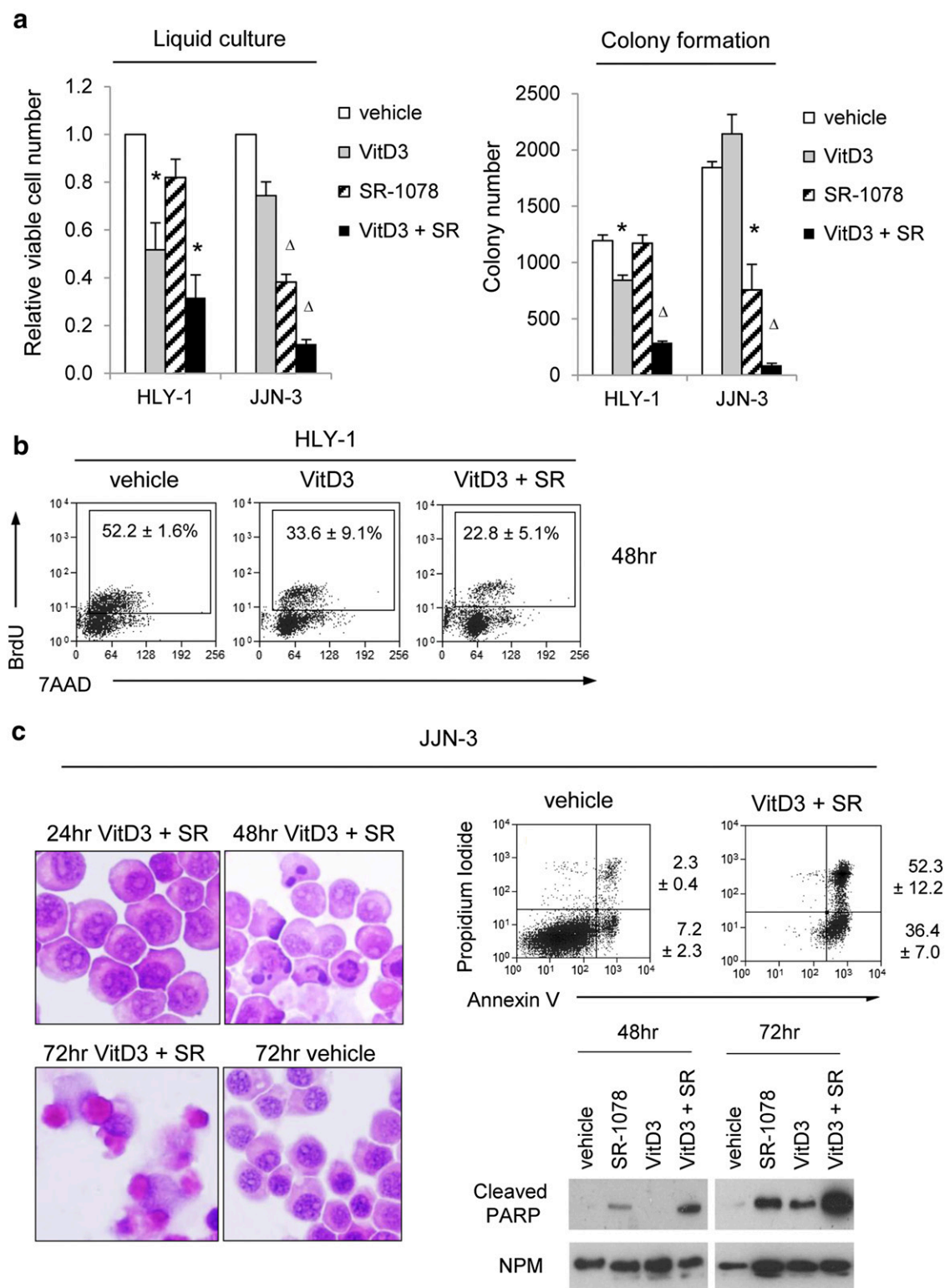


Figure 7. VitD3 effects on plasmablastic lymphoma cells can be enhanced by the synthetic ROR ligand SR-1078. (a, left panel) Relative viable cell number determined by MTS assay after 72-hour liquid culture with treatment indicated on right, $n = 4 \pm \text{SD}$. (a, right panel) Colony number after 7 days of semisolid methylcellulose culture containing treatments indicated, initiated after 24-hour liquid culture pretreatment, $n = 3 \pm \text{SE}$. (b) Flow cytometry of BrdU incorporation into, and 7-aminoactinomycin D (7-AAD) DNA content of, cells cultured 48 hours with treatments as indicated; numbers indicate mean percentage BrdU⁺, $n = 3 \pm \text{SD}$. (c, left panels) Morphology of JJN-3 treated with vehicle or combined VitD3 plus SR-1078 (VitD3 + SR), after cytospin and hematoxylin and eosin stain. (c, upper right panels) Annexin V/propidium iodide staining of unfixed JJN-3 72 hours after vehicle or VitD3 + SR-1078 treatment; numbers represent mean percentage of cells within right top (late apoptotic) and right bottom (early apoptotic) quadrants, $n = 3 \pm \text{SD}$. (c, lower right panels) Immunoblotting of cleaved poly ADP-ribose polymerase PARP in JJN-3 72 hours after treatment, representative of two experiments. SD, standard deviation; SE, standard error. * $P < 0.05$, $^{\Delta}P < 0.01$, comparisons to vehicle-treated samples.

Discussion

Here, by characterizing in detail a DLBCL cell line panel, we have identified a subset of ABC-DLBCL cell lines with plasmablastic features, most notably HLY-1. This included expression of VDR, which was present also in primary plasmablastic lymphoma and in myeloma cell lines. Manipulation of VitD3 levels and VDR expression can inhibit growth of lymphoma and myeloma cell lines, demonstrating this pathway to be biologically relevant.

Although VitD3 is widely recognized to inhibit growth, there are several indications that in plasmablastic cells, an endogenous VDR pathway promotes viability and/or growth. First, the proliferation of VDR⁺ cell lines HLY-1 and SU-DHL-9 is more vigorous *in vitro* than other DLBCL cell lines such as HBL-1 and OCI-Ly3 (D.M.G., unpublished observations). Second, VDR protein is expressed in dividing cells, and nuclear VDR positivity is associated with cell division in tumors and reduced upon growth inhibition. Thus, VDR expression positively associates with active cell division. Furthermore, direct VDR depletion reduces viable cell number. Overall, expression of CYP27B1 enabling local active VitD3 production, as demonstrated previously in a primary lymphoma case (22), and strong VDR autoregulation point toward a delicately balanced cell-intrinsic VitD3-VDR loop in plasmablastic lymphoma cells.

The clinical significance of circulating vitamin D levels in patients with lymphoma remains controversial. Our studies indicate that increasing active VitD3 concentration (*e.g.*, supplied via the circulation) might overstimulate the tumoral VDR pathway to inhibit growth and explain why lower circulating VitD3 levels can be associated with a poor outcome in myeloma (44) and DLBCL (27–30). Although these studies have partially excluded some or all overtly plasmablastic cases [*e.g.*, by selecting for CD20 positivity (27) or excluding HIV⁺ cases (29)], we believe such studies are likely to have included partially plasmablastic CD20⁺HIV[−]VDR⁺ tumors such as represented by the SU-DHL-9 cell line. A lack of association between circulating vitamin D levels and global lymphoma risk (26, 31) may result from a restricted tumoral VDR expression profile and/or from overriding importance of local vitamin D metabolism (45). Future studies might more robustly associate circulating vitamin D levels with lymphoma risk by segregating patients according to tumoral VDR expression.

Several studies have identified VDR coding-sequence polymorphism in lymphoma samples; thus, not only vitamin D and VDR levels but also the exact VDR form expressed may influence malignant plasmablastic cell biology and patient outcome. Specifically, VDR FOK1 polymorphism generates a variant lacking three amino

terminal amino acids, which our data associate with increased response to vitamin D, similar to some other studies (46). As with circulating VitD3, the variable impact of VDR polymorphism for lymphoma risk (23–25) may be defined by restricted tumoral expression of VDR. In contrast, our cell line expression data suggest that in myeloma, a significant association of FOK1 polymorphism with poor prognosis (47) might derive from increased protective VDR activity in the context of more widespread tumor cell VDR positivity.

Our findings demonstrate that VDR pathway manipulation might be of therapeutic relevance in plasmablastic lymphoma. First, given the protective effect of endogenous VDR on plasmablastic cells, inhibition using VDR antagonists (48, 49) may prove therapeutic, although effects on VDR⁺ normal tissues such as bone must be considered. Second, as we have undertaken *in vitro*, administration of vitamin D *in vivo* to patients with VDR⁺ disease might directly reduce tumor cell division, and in this regard, noncalcemic vitamin D analogues (18, 42) may prove of benefit. Third, our data suggest that although exogenous VitD3 is unable to completely arrest plasmablastic cell growth, it can sensitize to additional agents. Future investigations might productively examine the interactions of VitD3 and dexamethasone, which can activate VDR expression (50) or determine whether a positive impact of circulating vitamin D levels in rituximab-treated lymphoma (27) may derive from enhanced rituximab-mediated cytotoxicity.

Diagnosis of the relatively rare malignancy PBL currently depends on a combination of morphology and mixed B-cell and plasma cell surface marker expression (3, 4). However, improved characterization of plasmablastic phenotype is likely to identify additional plasmablastic ABC-DLBCL and myeloma cases that remain undetected using current diagnostic panels and unresponsive to existing therapies. VDR itself does not show sufficient differential expression between plasmablastic and nonplasmablastic DLBCL primary tumor cells to identify overt plasmablastic disease, and further research into tumoral HPGD, CTNNAL1, and/or IGF1 expression in DLBCL and myeloma may identify usual biomarkers of this type.

In summary, we have further demonstrated the utility of FOXP expression profiling in the characterization of malignant mature B-cell identity, specifically by establishing HLY-1 as an important cell line model with strongly plasmablastic characteristics. Our data indicate potentially conserved vitamin D pathway activity in plasmablastic subsets of both lymphoma and myeloma, and further characterization and manipulation of this pathway may enable improved diagnostic and therapeutic interventions in this difficult disease.

Acknowledgments

The authors thank Dr Giovanna Roncador for the gift of anti-PRDM1 antibody and Shazia Irshad and Demin Li for useful discussions.

Address all correspondence and requests for reprints to: Alison Banham, DPhil (Oxon), FRCPATH, Nuffield Division of Clinical Laboratory Sciences, Radcliffe Department of Medicine, University of Oxford, Level 4 Academic Block, John Radcliffe Hospital, Headington, Oxford, OX3 9DU, United Kingdom. E-mail: alison.banham@ndcls.ox.ac.uk.

D.M.G., L.L., H.S., and E.J.S. were supported by Specialist Program Grants (Ref:10044, 13047) to A.H.B. from Bloodwise and the National Institute for Health Research Oxford Biomedical Research Centre program.

Disclosure Summary: The authors have nothing to disclose.

References

- Pasqualucci L, Dalla-Favera R. SnapShot: diffuse large B cell lymphoma. *Cancer Cell*. 2014;25:132–132.e131.
- Wilkinson ST, Vanpatten KA, Fernandez DR, Brunhoeber P, Garsha KE, Glinsmann-Gibson BJ, Grogan TM, Teruya-Feldstein J, Rimsza LM. Partial plasma cell differentiation as a mechanism of lost major histocompatibility complex class II expression in diffuse large B-cell lymphoma. *Blood*. 2011;119(6):1459–1467.
- Castillo JJ, Bibas M, Miranda RN. The biology and treatment of plasmablastic lymphoma. *Blood*. 2015;125(15):2323–2330.
- Montes-Moreno S, Montalbán C, Piris MA. Large B-cell lymphomas with plasmablastic differentiation: a biological and therapeutic challenge. *Leuk Lymphoma*. 2011;53(2):185–194.
- Rajkumar SV, Fonseca R, Lacy MQ, Witzig TE, Therneau TM, Kyle RA, Litzow MR, Gertz MA, Greipp PR. Plasmablastic morphology is an independent predictor of poor survival after autologous stem-cell transplantation for multiple myeloma. *J Clin Oncol*. 1999;17(5):1551–1557.
- Johnston AC, Naresh K, Barwick T, May P, Karadimitris A, Auner HW. Cutaneous presentation of an aggressive plasmablastic neoplasm indiscriminate between lymphoma and myeloma. *Ann Hematol*. 2014;94(4):691–692.
- Mondal SK, Bera H, Biswas PK, Mallick MG. High-grade plasmablastic neoplasm of humerus in an HIV-negative patient, which was indeterminate between plasmablastic lymphoma and plasmablastic myeloma. *J Cancer Res Ther*. 2011;7(2):214–216.
- Cocco M, Stephenson S, Care MA, Newton D, Barnes NA, Davison A, Rawstron A, Westhead DR, Doody GM, Tooze RM. In vitro generation of long-lived human plasma cells. *J Immunol*. 2012;189(12):5773–5785.
- Jourdan M, Caraux A, Caron G, Robert N, Fioll G, Rème T, Bolloré K, Vendrell JP, Le Gallou S, Mourcin F, De Vos J, Kassambara A, Duperray C, Hose D, Fest T, Tarte K, Klein B. Characterization of a transitional preplasmablast population in the process of human B cell to plasma cell differentiation. *J Immunol*. 2011;187(8):3931–3941.
- Brown PJ, Campbell AJ, Lyne L, Chi J, Lawrie CH, Kusé R, Banham AH. Expression of the FOXP1 transcription factor is post-transcriptionally silenced in normal and malignant CD138+ plasma cells. *Open Leukemia J*. 2009;2:32–39.
- Matsuki E, Miyakawa Y, Asakawa S, Tsukada Y, Yamada T, Yokoyama K, Kudoh J, Ikeda Y, Okamoto S. Identification of loss of p16 expression and upregulation of MDR-1 as genetic events resulting from two novel chromosomal translocations found in a plasmablastic lymphoma of the uterus. *Clin Cancer Res*. 2011;17:2101–2109.
- Nichele I, Zamò A, Bertolaso A, Bifari F, Tinelli M, Franchini M, Stradoni R, Aprili F, Pizzolo G, Krampera M. VR09 cell line: an EBV-positive lymphoblastoid cell line with in vivo characteristics of diffuse large B cell lymphoma of activated B-cell type. *PLoS One*. 2012;7(12):e52811.
- Heine G, Niesner U, Chang HD, Steinmeyer A, Zügel U, Zuberbier T, Radbruch A, Worm M. 1,25-Dihydroxyvitamin D(3) promotes IL-10 production in human B cells. *Eur J Immunol*. 2008;38(8):2210–2218.
- Morgan JW, Reddy GS, Uskokovic MR, May BK, Omdahl JL, Maizel AL, Sharma S. Functional block for 1 alpha,25-dihydroxyvitamin D3-mediated gene regulation in human B lymphocytes. *J Biol Chem*. 1994;269(18):13437–13443.
- Morgan JW, Morgan DM, Lasky SR, Ford D, Kouttab N, Maizel AL. Requirements for induction of vitamin D-mediated gene regulation in normal human B lymphocytes. *J Immunol*. 1996;157(7):2900–2908.
- Provvedini DM, Tsoukas CD, Deftos LJ, Manolagas SC. 1,25-Dihydroxyvitamin D3 receptors in human leukocytes. *Science*. 1983;221(4616):1181–1183.
- Chen WC, Vayuvegula B, Gupta S. 1,25-Dihydroxyvitamin D3-mediated inhibition of human B cell differentiation. *Clin Exp Immunol*. 1987;69(3):639–646.
- Kumagai T, O'Kelly J, Said JW, Koeffler HP. Vitamin D2 analog 19-nor-1,25-dihydroxyvitamin D2: antitumor activity against leukemia, myeloma, and colon cancer cells. *J Natl Cancer Inst*. 2003;95(12):896–905.
- Park WH, Seol JG, Kim ES, Jung CW, Lee CC, Binderup L, Koeffler HP, Kim BK, Lee YY. Cell cycle arrest induced by the vitamin D(3) analog EB1089 in NCI-H929 myeloma cells is associated with induction of the cyclin-dependent kinase inhibitor p27. *Exp Cell Res*. 2000;254(2):279–286.
- Hickish T, Cunningham D, Colston K, Millar BC, Sandle J, Mackay AG, Soukop M, Sloane J. The effect of 1,25-dihydroxyvitamin D3 on lymphoma cell lines and expression of vitamin D receptor in lymphoma. *Br J Cancer*. 1993;68(4):668–672.
- Renné C, Benz AH, Hansmann ML. Vitamin D3 receptor is highly expressed in Hodgkin's lymphoma. *BMC Cancer*. 2012;12:215.
- Mudde AH, van den Berg H, Boshuis PG, Breedveld FC, Markusse HM, Kluin PM, Bijvoet OL, Papapoulos SE. Ectopic production of 1,25-dihydroxyvitamin D by B-cell lymphoma as a cause of hypercalcemia. *Cancer*. 1987;59(9):1543–1546.
- Smedby KE, Eloranta S, Duvefelt K, Melbye M, Humphreys K, Hjalgrim H, Chang ET. Vitamin D receptor genotypes, ultraviolet radiation exposure, and risk of non-Hodgkin lymphoma. *Am J Epidemiol*. 2010;173(1):48–54.
- Kelly JL, Drake MT, Fredericksen ZS, Asmann YW, Liebow M, Shanafelt TD, Feldman AL, Ansell SM, Macon WR, Herr MM, Wang AH, Nowakowski GS, Call TG, Habermann TM, Slager SL, Witzig TE, Cerhan JR. Early life sun exposure, vitamin D-related gene variants, and risk of non-Hodgkin lymphoma. *Cancer Causes Control*. 2012;23(7):1017–1029.
- Purdue MP, Lan Q, Krickler A, Vajdic CM, Rothman N, Armstrong BK. Vitamin D receptor gene polymorphisms and risk of non-Hodgkin's lymphoma. *Haematologica*. 2007;92(8):1145–1146.
- Łuczyńska A, Kaaks R, Rohrmann S, Becker S, Linseisen J, Buijsse B, Overvad K, Trichopoulou A, Valanou E, Barmptsioti A, Masala G, Agnoli C, Tumino R, Panico S, Bueno-de-Mesquita HB, van Duynhoven FJ, Peeters PH, Vermeulen R, Weiderpass E, Brustad M, Skeie G, González CA, Jakšzyn P, Quirós JR, Sánchez MJ, Huerta JM, Ardanaz E, Melin B, Johansson AS, Almqvist M, Malm J, Khaw KT, Wareham N, Travis RC, Fedirko V, Romieu I, Jenab M, Gallo V, Riboli E, Vineis P, Nieters A. Plasma 25-hydroxyvitamin D concentration and lymphoma risk: results of the European Prospective Investigation into Cancer and Nutrition. *Am J Clin Nutr*. 2013;98(3):827–838.
- Bittenbring JT, Neumann F, Altmann B, Achenbach M, Reichrath J, Ziepert M, Geisel J, Regitz E, Held G, Pfreundschuh M. Vitamin D

- deficiency impairs rituximab-mediated cellular cytotoxicity and outcome of patients with diffuse large B-cell lymphoma treated with but not without rituximab. *J Clin Oncol.* 2014;**32**(29):3242–3248.
28. Vaidya R, Witzig TE. Prognostic factors for diffuse large B-cell lymphoma in the R(X)CHOP era. *Ann Oncol.* 2014;**25**(11):2124–2133.
 29. Drake MT, Maurer MJ, Link BK, Habermann TM, Ansell SM, Micallef IN, Kelly JL, Macon WR, Nowakowski GS, Inwards DJ, Johnston PB, Singh RJ, Allmer C, Slager SL, Weiner GJ, Witzig TE, Cerhan JR. Vitamin D insufficiency and prognosis in non-Hodgkin's lymphoma. *J Clin Oncol.* 2010;**28**(27):4191–4198.
 30. Wang W, Li G, He X, Gao J, Wang R, Wang Y, Zhao W. Serum 25-hydroxyvitamin D levels and prognosis in hematological malignancies: a systematic review and meta-analysis. *Cell Physiol Biochem.* 2015;**35**(5):1999–2005.
 31. Lu D, Chen J, Jin J. Vitamin D status and risk of non-Hodgkin lymphoma: a meta-analysis. *Cancer Causes Control.* 2014;**25**(11):1553–1563.
 32. Brown PJ, Ashe SL, Leich E, Burek C, Barrans S, Fenton JA, Jack AS, Pulford K, Rosenwald A, Banham AH. Potentially oncogenic B-cell activation-induced smaller isoforms of FOXP1 are highly expressed in the activated B cell-like subtype of DLBCL. *Blood.* 2007;**111**(5):2816–2824.
 33. Lenz G, Wright G, Dave SS, Xiao W, Powell J, Zhao H, Xu W, Tan B, Goldschmidt N, Iqbal J, Vose J, Bast M, Fu K, Weisenburger DD, Greiner TC, Armitage JO, Kyle A, May L, Gascoyne RD, Connors JM, Troen G, Holte H, Kvaloy S, Dierickx D, Verhoef G, Delabie J, Smeland EB, Jares P, Martinez A, Lopez-Guillermo A, Montserrat E, Campo E, Braziel RM, Miller TP, Rimsza LM, Cook JR, Pohlman B, Sweetenham J, Tubbs RR, Fisher RI, Hartmann E, Rosenwald A, Ott G, Muller-Hermelink HK, Wrench D, Lister TA, Jaffe ES, Wilson WH, Chan WC, Staudt LM; Lymphoma/Leukemia Molecular Profiling Project. Stromal gene signatures in large-B-cell lymphomas. *N Engl J Med.* 2008;**359**(22):2313–2323.
 34. Hu H, Wang B, Borde M, Nardone J, Maika S, Allred L, Tucker PW, Rao A. Foxp1 is an essential transcriptional regulator of B cell development. *Nat Immunol.* 2006;**7**(8):819–826.
 35. Ngo VN, Young RM, Schmitz R, Jhavar S, Xiao W, Lim KH, Kohlhammer H, Xu W, Yang Y, Zhao H, Shaffer AL, Romesser P, Wright G, Powell J, Rosenwald A, Muller-Hermelink HK, Ott G, Gascoyne RD, Connors JM, Rimsza LM, Campo E, Jaffe ES, Delabie J, Smeland EB, Fisher RI, Braziel RM, Tubbs RR, Cook JR, Weisenburger DD, Chan WC, Staudt LM. Oncogenically active MYD88 mutations in human lymphoma. *Nature.* 2010;**470**(7332):115–119.
 36. Fontan L, Yang C, Kabaleeswaran V, Volpon L, Osborne MJ, Beltran E, Garcia M, Cerchietti L, Shaknovich R, Yang SN, Fang F, Gascoyne RD, Martinez-Climent JA, Glickman JF, Borden K, Wu H, Melnick A. MALT1 small molecule inhibitors specifically suppress ABC-DLBCL in vitro and in vivo. *Cancer Cell.* 2012;**22**(6):812–824.
 37. Ceribelli M, Kelly PN, Shaffer AL, Wright GW, Xiao W, Yang Y, Mathews Griner LA, Guha R, Shinn P, Keller JM, Liu D, Patel PR, Ferrer M, Joshi S, Nerle S, Sandy P, Normant E, Thomas CJ, Staudt LM. Blockade of oncogenic I κ B kinase activity in diffuse large B-cell lymphoma by bromodomain and extraterminal domain protein inhibitors. *Proc Natl Acad Sci USA.* 2014;**111**(31):11365–11370.
 38. Rossi JF, Durie BG, Duperray C, Braich T, Marion SL, Pike JW, Haussler MR, Janbon C, Bataille R. Phenotypic and functional analysis of 1,25-dihydroxyvitamin D3 receptor mediated modulation of the human myeloma cell line RPMI 8226. *Cancer Res.* 1988;**48**(5):1213–1216.
 39. Solt LA, Kumar N, Nuhant P, Wang Y, Lauer JL, Liu J, Istrate MA, Kamenecka TM, Roush WR, Vidović D, Schürer SC, Xu J, Wagoner G, Drew PD, Griffin PR, Burris TP. Suppression of TH17 differentiation and autoimmunity by a synthetic ROR ligand. *Nature.* 2011;**472**(7344):491–494.
 40. Wang Y, Solt LA, Kojetin DJ, Burris TP. Regulation of p53 stability and apoptosis by a ROR agonist. *PLoS One.* 2012;**7**(4):e34921.
 41. Wang Y, Becklund BR, DeLuca HF. Identification of a highly specific and versatile vitamin D receptor antibody. *Arch Biochem Biophys.* 2010;**494**(2):166–177.
 42. Kozielwicz P, Grafton G, Kutner A, Curnow SJ, Gordon J, Barnes NM. Novel vitamin D analogues: cytotoxic and anti-proliferative activity against a diffuse large B-cell lymphoma cell line and B-cells from healthy donors. *J Steroid Biochem Mol Biol.* 2016;**164**:98–105.
 43. Reitsma PH, Rothberg PG, Astrin SM, Trial J, Bar-Shavit Z, Hall A, Teitelbaum SL, Kahn AJ. Regulation of myc gene expression in HL-60 leukaemia cells by a vitamin D metabolite. *Nature.* 1983;**306**(5942):492–494.
 44. Ng AC, Kumar SK, Rajkumar SV, Drake MT. Impact of vitamin D deficiency on the clinical presentation and prognosis of patients with newly diagnosed multiple myeloma. *Am J Hematol.* 2009;**84**(7):397–400.
 45. Adams JS, Rafison B, Witzel S, Reyes RE, Shieh A, Chun R, Zavala K, Hewison M, Liu PT. Regulation of the extrarenal CYP27B1-hydroxylase. *J Steroid Biochem Mol Biol.* 2014;**144**(Pt A):22–27.
 46. Whitfield GK, Remus LS, Jurutka PW, Zitzer H, Oza AK, Dang HT, Haussler CA, Galligan MA, Thatcher ML, Encinas Dominguez C, Haussler MR. Functionally relevant polymorphisms in the human nuclear vitamin D receptor gene. *Mol Cell Endocrinol.* 2001;**177**(1–2):145–159.
 47. Shafia S, Qasim I, Aziz SA, Bhat IA, Nisar S, Shah ZA. Role of vitamin D receptor (VDR) polymorphisms in susceptibility to multiple myeloma in ethnic Kashmiri population. *Blood Cells Mol Dis.* 2013;**51**(1):56–60.
 48. Hartmann B, Heine G, Babina M, Steinmeyer A, Zügel U, Radbruch A, Worm M. Targeting the vitamin D receptor inhibits the B cell-dependent allergic immune response. *Allergy.* 2010;**66**(4):540–548.
 49. Sakamaki Y, Inaba Y, Yoshimoto N, Yamamoto K. Potent antagonist for the vitamin D receptor: vitamin D analogues with simple side chain structure. *J Med Chem.* 2010;**53**(15):5813–5826.
 50. Hidalgo AA, Deeb KK, Pike JW, Johnson CS, Trump DL. Dexamethasone enhances 1 α ,25-dihydroxyvitamin D3 effects by increasing vitamin D receptor transcription. *J Biol Chem.* 2011;**286**(42):36228–36237.